CHAPTER IV

RESULTS AND DISCUSSION

4.1 Production of residue glycerine from transesterification of *Jatropha curcas* oil

The *Jatropha curcas* oil was transesterified with methanol in the presence of NaOH. Two layers were formed; the bottom layer was residue glycerine and the top layer was the methyl ester, as shown in Figure 4.1. The yield of this process was 73.34% methyl ester by weight from the starting oil of 25.46% residue glycerine, The results are shown in Figure 4.1 and Table 4.1. The yield in this study was relatively less than those previously reported for methyl esters of *Jatropha curcas* oil (92% of theoretical yield) and other vegetable oils. Under the same conditions, 67-87% conversion using crude vegetable oils, compared with 94-97% when using refined oil (Srivastava and Prasad, 2000). Besides the reactant purity, the ratio of alcohol to oil, catalyst type and concentration and mixing intensity also influence the ester yield.

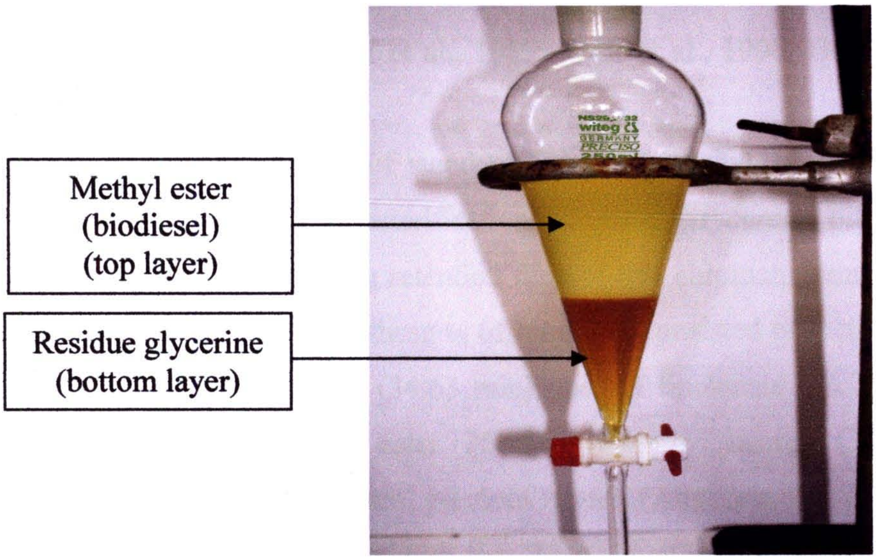

Figure 4.1 Transesterification process of *Jatropha curcas* oil

Table 4.1 Percentage of methyl ester and residue glycerine

No. samples	**% methyl esters**	**% residue glycerine**
1	74.32	25.68
2	74.58	25.42
3	74.34	25.66
Average	74.41	25.59
± SD	0.14	0.14

4.2 The composition analysis of biodiesel from transesterification of *Jatropha curcas* oil

Using the optimal temperature program, the analysis was achieved within 65 min. A fatty acid methyl ester mixture was performed and retention times were monitored for identifying these sample peaks. Fatty acid levels were estimated as percentage of total peak area of methyl esters. The fatty acid methyl ester composition of biodiesel was compared with some previous reported values. The fatty acid methyl esters found common in oil samples were methyl palmitate, methyl palmitoleate, methyl stearate, oleic methyl ester, methyl linoleate. The results obtained are very similar to these reports (Banerji et al., 1985; Foidl et al., 1996; Gubitz et al., 1999; Nasir et al., 1988).

GC-MS chromatogram of standard fatty acid methyl ester (Figure 4.3.) and biodiesel obtained from transesterification of *Jatropha curcas* oil are shown in Figure 4.3. Based on comparing retention time of this chromatogram as summarized in Table 4.2, it was found that these t_R of biodiesel consisted of methyl palmitoleate (32.25 min), Methyl palmitate (34.63 min), methyl linolenate (36.27 min), methyl linoleate (36.51), oleic methyl ester (36.53) and methyl stearate (36.96 min). Our results were correlated with several previous reports (Augustus et al., 2002; Akintaya, 2004; Openshaw, 2000). They present that the main composition of *Jatropha curcas* oil were methyl palmitate, methyl palmitoleate, methyl stearate, oleic methyl ester, methyl linoleate. Moreover, the results in Table 4.2 implied that this reaction can be produced both biodiesel and glycerine.

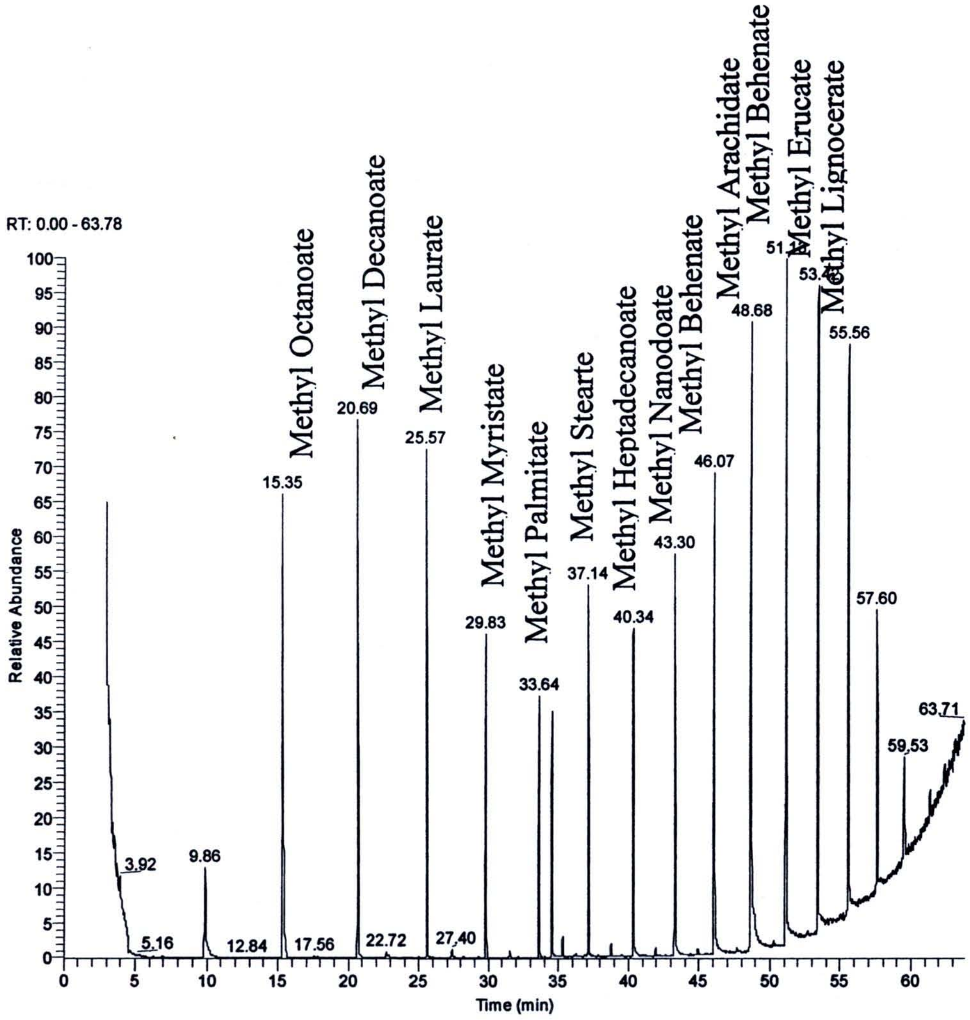

Figure 4.2 GC-MS chromatogram of standard fatty acid methyl ester

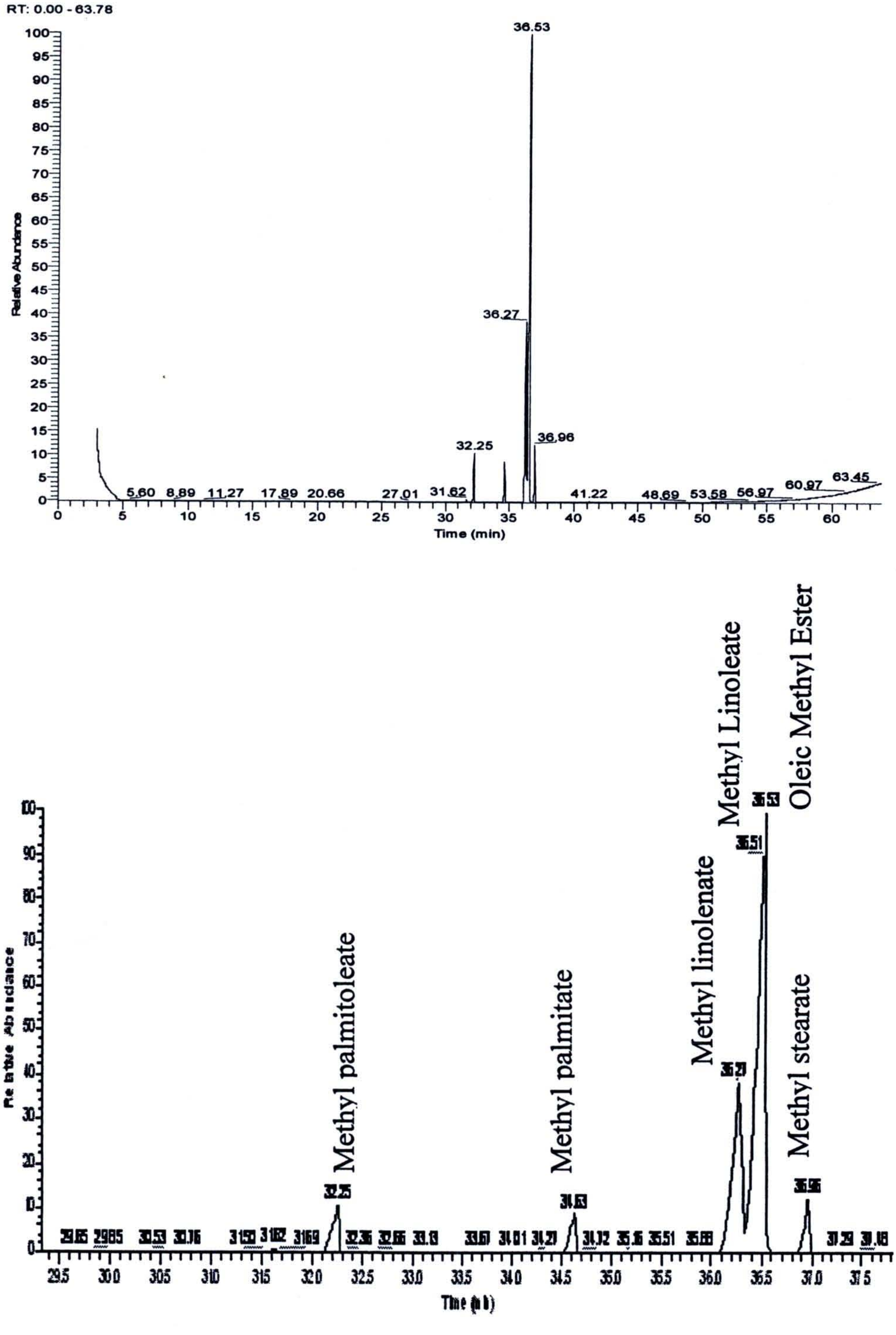

Figure 4.3 Biodiesel obtained from transesterification of *Jatropha curcas* oil

Table 4.2 The composition of biodiesel from transesterification of *Jatropha curcas* Oil by GC-MS

Composition	t_R (min)
Methyl palmitoleate	32.25
Methyl palmitate	34.63
Methyl linolenate	36.27
Methyl linoleate	36.51
Oleic methyl ester	36.53
Methyl stearate	36.96

4.3 Purification of residue glycerine from transesterification of *Jatropha curcas* oil

4.3.1 Purification of residue glycerine by conventional method

Chemical compositions of glycerine standard and residue glycerine are presented in Table 4.3. It was found that the purity of residue glycerine obtained from transesterification of *Jatropha curcas* oil (50.05%) was relatively low when compared with standard glycerine (99.50%).

Table 4.3 Chemical compositions of standard glycerine and residue glycerine

No. samples	Glycerine (%)	Ash (%)	Water (%)	MONG (%)	Density (g/cm^3)	pH
Standard glycerine	99.50	0.001	0.44	0.025	1.25	6.86
Residue glycerine	50.05	23.71	9.98	16.26	0.81	10.11

FT-IR spectra of standard glycerine and residue glycerine obtained from transesterification of *Jatropha curcas* oil are shown in Figure 4.4. The presence of OH group in all samples was evidenced by fundamental mode of O-H stretching at 3387 cm^{-1}. It was found C-H stretching at 2890 and 2942 cm^{-1}. The presence of some impurities was shown by the absorption peak at 1648 cm^{-1} (C=O group). Furthermore, C-O stretching from 1043 to 1120 cm^{-1} and O-H bending at 924 cm^{-1} were observed in FT-IR spectra of standard glycerine. FT-IR spectra of standard glycerine and residue glycerine obtained from transesterification of *Jatropha curcas* oil also showed almost similar absorption patterns but present a broader absorption band at 3387.93 cm^{-1}. This was probably due to the result of hydroxyl groups from water. It was indicated that showed the presence of residue glycerine and some impurities during 1200 to 1800 cm^{-1}. This residue glycerine still contained the impurity compounds on spectra that appeared from high salts, free fatty acid contents and substantial color.

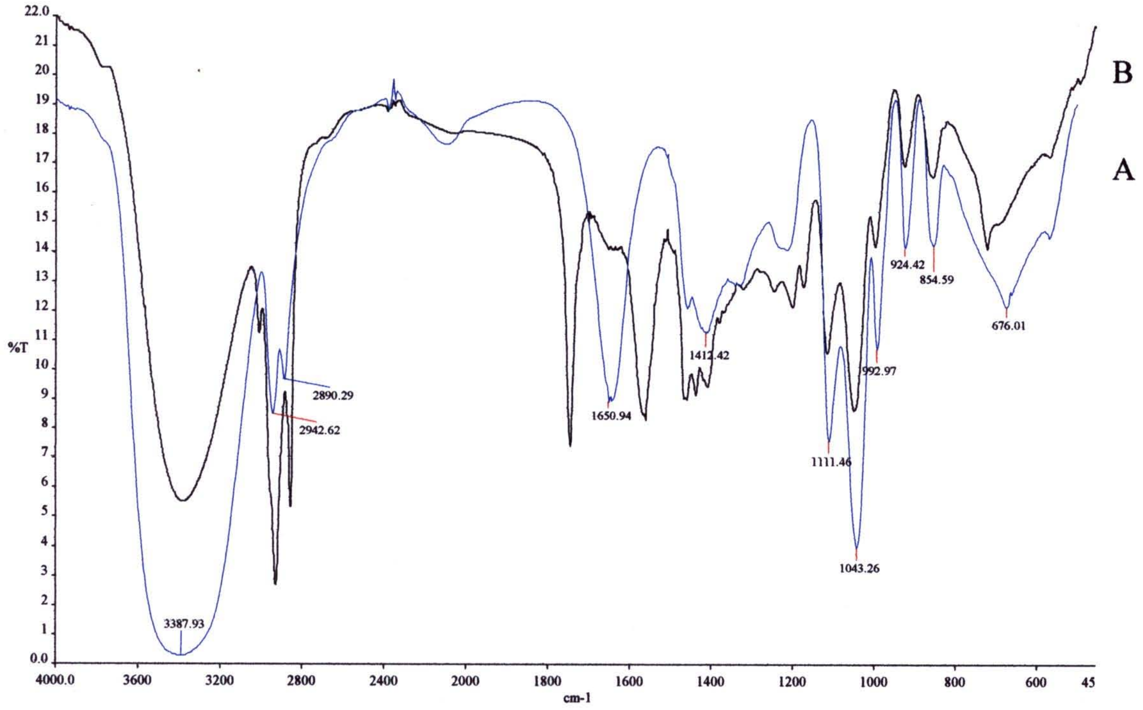

Figure 4.4 FT-IR spectra of standard glycerine (A) and residue glycerine (B)

One initial step common to all glycerine purification process that all fat, soap and other organic impurities need to be chemically separated and removed by using 6% sulfuric acid to split the soap, and neutralize the residual NaOH. By variation of dilute sulfuric acid amounts used in the acidification of residue glycerine were pH value of 1, 2, 3, 4, 5 and 6 respectively, are summarized in Table 4.4 and Figure 4.5. Effect of pH in the chemical and physical treatments on the composition of residue glycerine is shown in Figure 4.5. As high pH 5-6 increased charred substance, viscose liquid, difficulty filtered at the present pH but for other charred substance solids was easily filtered. The charred substance at pH 5-6 obtained was soap, fatty acids and glyceride. Therefore, percentage of isolated compounds from residue glycerine decreased as different pH values. While, at the pH 1 increased the dissolved salt because of the salting out of acid for adjusts pH. So, increasing of purified glycerine was at the pH 3 and percentage of purified glycerine was up to 40%, as shown in Table 4.4.

Table 4.4 Compositions percentage (w/w) of isolated from residue glycerine in different pH value

pH	Compositions percentage (w/w) of isolated from residue glycerine			
	purified glycerine	fatty acids	Charred substance	Salt
1	35.71	31.34	7.98	10.01
2	37.85	30.61	7.75	8.65
3	40.18	31.42	7.47	6.87
4	39.23	32.09	7.56	5.94
5	35.65	29.87	9.45	5.58
6	34.45	30.51	10.98	5.76

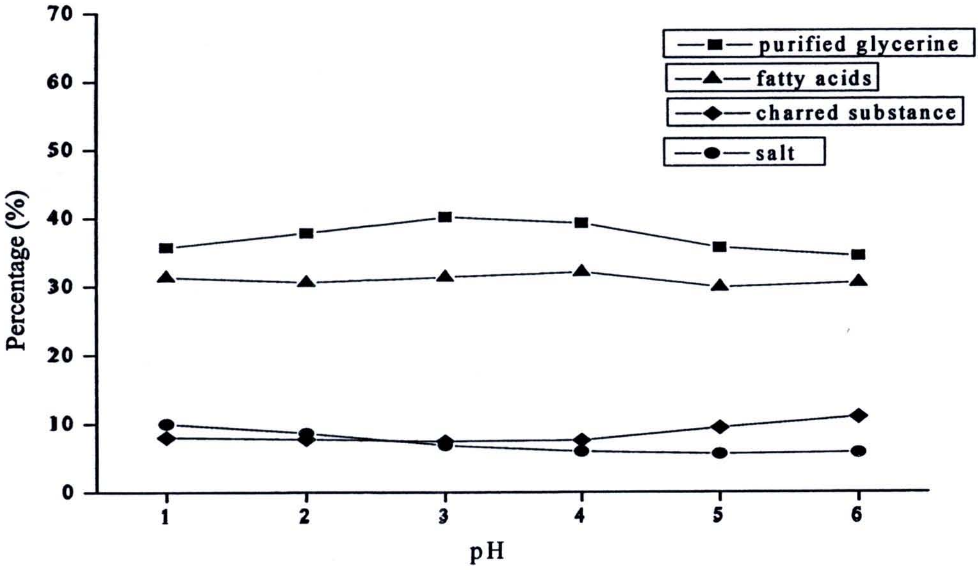

Figure 4.5 Effect of pH in the chemical and physical treatments on the composition of purified glycerine

Chemical compositions of purified glycerine from conventional method are summarized in Table 4.5. The analysis showed that the average compositions of the purified glycerine obtained were: 70.35% glycerol, 12.92% ash, 10.76% water and 5.97% MONG. It was observed that the glycerine content of purified glycerine process was increased while compared with residue glycerine in some reports (as 90% glycerine content, Tovbin et al., 2005; 96.6% glycerine content, Yong et al., 2001; 80% glycerine content, Hazinah et al., 2003). However, water content was slightly increased. It probably due to glycerol is hygroscopic, thus it absorbs moisture from its surrounding. On the other hands, ash content and MONG were decreased when compared with residue glycerine because salts (NaCl and Na_2SO_4) mainly constituted the ash. They were removed by acidification and neutralization steps in conventional method. In addition, residue glycerine contained some organic matters including soap and methyl esters which can be also removed by acidification step.

Table 4.5 Chemical compositions of purified glycerine obtained by conventional method

No. samples	**Glycerine (%)**	**Ash (%)**	**Water (%)**	**MONG (%)**	**Density (g/cm^3)**	**pH**
1	70.01	12.89	10.56	6.54	1.37	6.92
2	70.75	12.92	10.84	5.49	1.02	6.21
3	70.29	12.95	10.89	5.87	1.27	6.60
Average	70.35	12.92	10.76	5.97	1.22	6.57

FT-IR spectra of standard glycerine and purified glycerine obtained conventional method are shown in Figure 4.6. The presence of OH group in all samples was evidenced by fundamental mode of O-H stretching at 3400 cm^{-1}. It was found in C-H stretching at 2890 and 2942 cm^{-1}. The presence of some impurities was shown by the absorption peak at 1650 cm^{-1} (C=O group). The glycerol moiety of the standard glycerine is evidenced by the absorption peak at 1400 to 1460 cm^{-1}, assigned to overlapping of the CH in-planed and O-H bending in the glycerol molecule. Furthermore, C-O stretching from 1043 to 1120 cm^{-1} and O-H bending at 924 cm^{-1} were observed in FT-IR spectra of standard glycerine. FT-IR spectra of standard glycerine and purified glycerine obtained by conventional method showed almost similar absorption patterns but with a broader absorption band at 3387 cm^{-1} and 1043 to 1400 cm^{-1}. This was probably due to the hydroxyl groups of water, high salts from acid for pH adjustment and ash content.

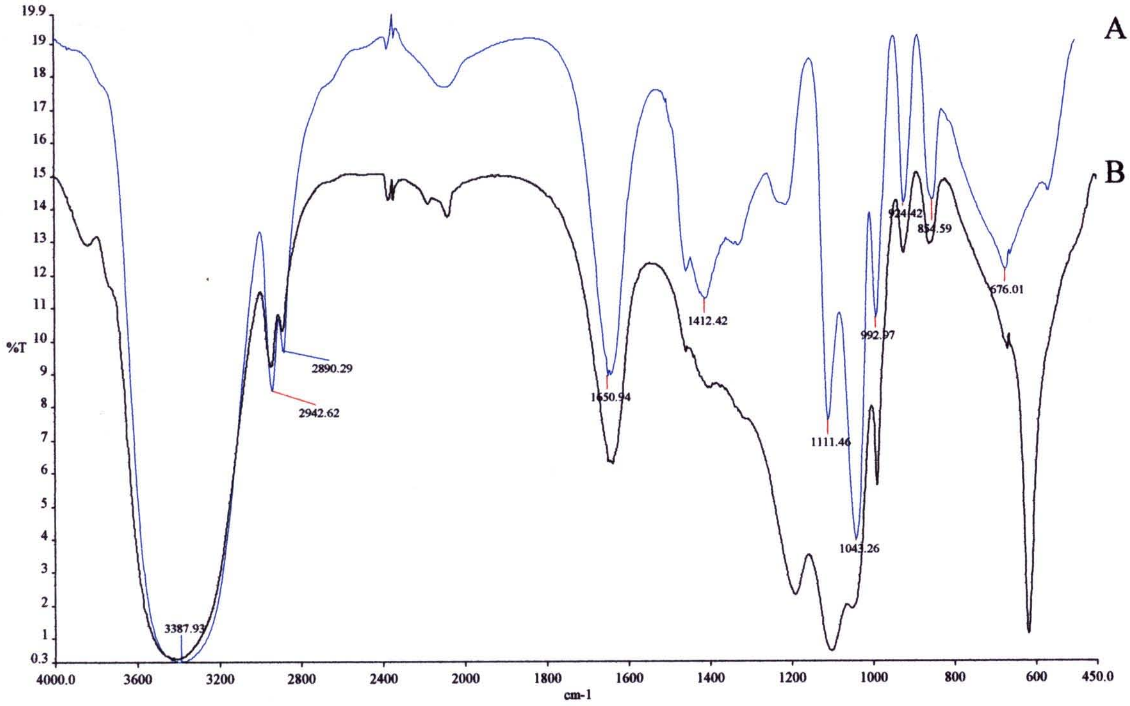

Figure 4.6 FT-IR spectra of standard glycerine (A) and purified glycerine obtained by conventional method (B)

4.3.2 Purification of residue glycerine by improved method

4.3.2.1 Study on optimization conditions for purification of residue glycerine solution by mixed with cation exchange resin

Improved method was performed as following step: acidifycation by adding 1 M sulfuric acid to split the soap and neutralize the residual NaOH. Subsequently, the glycerine solution was mixed with cation exchange resin. By this method, the optimization condition was investigated. The varying parameters studied were ratio of cation exchange resin to residue glycerine (1:1, 1:2, 1:3 and 1:4 w/w), contacting time (30, 60, 90, 120 and 180 min) and agitation rate (0, 50, 100, 150 and 200 rpm). The eluates obtained from batch experiment were then evaporated to remove methanol. The final products were also called purified glycerine. The results of optimization conditions for purification of residue glycerine solution mixed with cation exchange resin are demonstrated in Figure 4.7 - 4.9. It was indicated that the optimized conditions for batch experiment were 1:3 (w/w) of ratio of cation exchanger resin to glycerine for 90 min of contacting time and 50 rpm of agitation rate, respectively. The purified glycerine in this optimized conditions by mixed with cation exchange resin comprised 74.25% glycerine, 10.95% ash, 9.69% water and 5.11% MONG as summarized in Table 4.6. The results in Table 4.6 suggested that the improved method had effectively removed the impurities in glycerine residue. because cation exchange resin can exchange some positive charge ions from ionization of salts and others, constituted the ash. Therefore, ash content decreased resulting in the higher purity of glycerine was obtained by improved method. Moreover, MONG comprised mainly partial glycerides, free fatty acid, oxidation products and the polymerized compounds of glycerine, were reduced because of some MONG removal by prior acidification step.

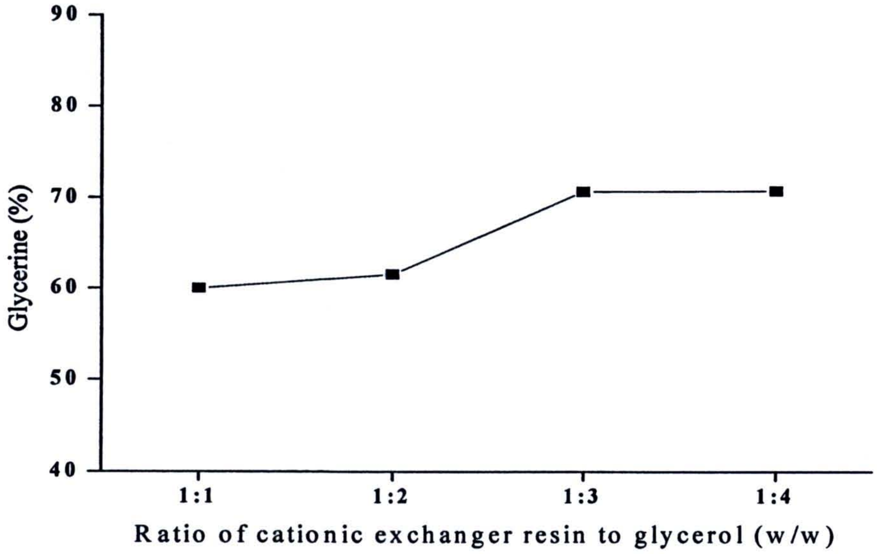

Figure 4.7 Effect of the ratio of cation exchange resin to glycerine on percentage of glycerine content

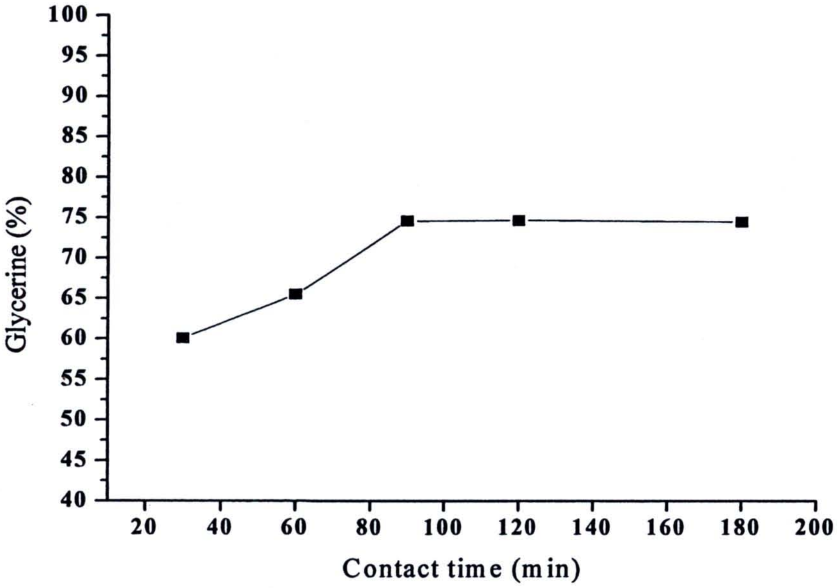

Figure 4.8 Effect of contact time of cation exchange resin to glycerine on percentage of glycerine content

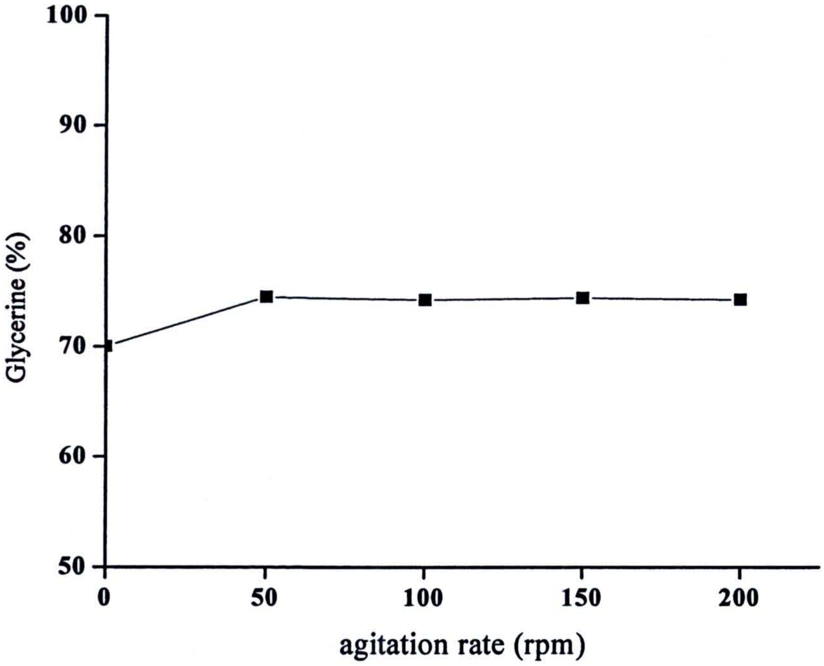

Figure 4.9 Effect of agitation rate of cation exchange resin to glycerine on percentage of glycerine content

Table 4.6 Chemical compositions of purified glycerine obtained from optimized conditions of residue glycerine solution by mixed with cation exchange resin

No. samples	Glycerine (%)	Ash (%)	Water (%)	MONG (%)	Density (g/cm^3)	pH
1	74.35	10.85	9.85	5.05	1.19	6.97
2	74.13	10.83	9.62	5.18	1.26	6.71
3	74.27	11.17	9.59	5.10	1.24	6.85
Average	74.25	10.95	9.69	5.11	1.23	6.84

FT-IR spectra of standard glycerine and purified glycerine obtained from purification of residue glycerine solution by mixed with cation exchanger resin are expressed as shown in Figure 4.10. The presence of OH group in all samples was evidenced by fundamental mode of O-H stretching at 3400 cm^{-1}. It was found that C-H stretching at 2880 and 2940 cm^{-1}. The presence of some impurities was shown by the absorption peak at 1648 cm^{-1} (C=O group). The glycerol moiety of the standard glycerine is evidenced by the absorption peak at 1400 to 1460 cm^{-1}, assigned to overlapping of the CH in-planed and O-H bending in the glycerol molecule. Furthermore, C-O stretching from 1040 to 1120 cm^{-1} and O-H bending at 920 cm^{-1} were observed in FT-IR spectra of standard glycerine. FT-IR spectra of glycerine standard and purified glycerine obtained from purification of residue glycerine solution were mixed with cation exchange resin also showed almost similar absorption patterns but still represent a broader absorption band at 3387 cm^{-1}. This was probably due to the hydroxyl groups from water.

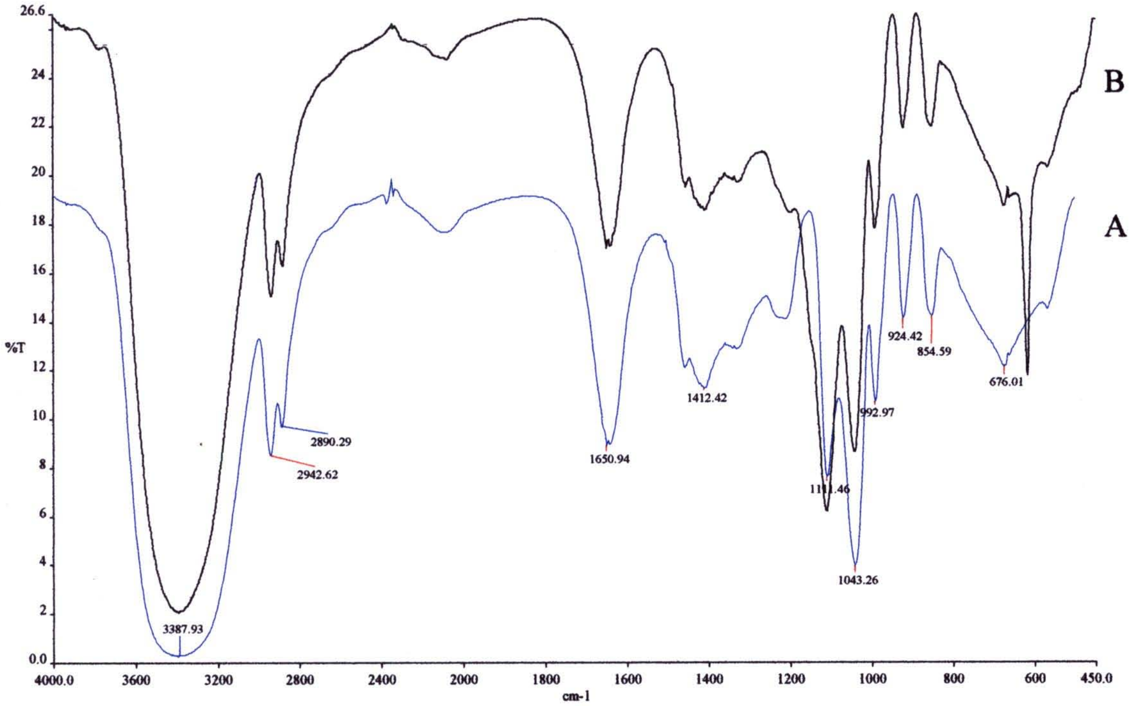

Figure 4.10 FT-IR spectra of standard glycerine (A) and improved method of residue glycerine solution by mixed with cation exchange resin (B)

4.3.2.2 Study of optimization conditions for purification of residue glycerine solution by mixed with anion exchange resin

Next parameters variation studied was ratio of anion exchange resin to residue glycerine solution (in ratio 1:1, 1:2, 1:3 and 1:4 w/w), contacting time (30, 60, 90, 120 and 180 min) and agitation rate (0, 50, 100, 150 and 200 rpm). Each eluate obtained batch experiment was then evaporated to remove methanol. The final products were so called purified glycerine. The results of optimization conditions for purification of residue glycerine solution were used by mixed with anion exchange resin as shown in Figure 4.11 - 4.13. It was indicated that these optimized conditions for batch experiment obtained were 1:3(w/w) of ratio of anion exchange resin to glycerine, 90 min of contacting time and 50 rpm of agitation rate, respectively. The purified glycerine obtained by mixed with anion exchange resin comprised 74.58% glycerine, 10.68% ash, 9.78% water and 5.36% MONG are summarized in Table 4.7.

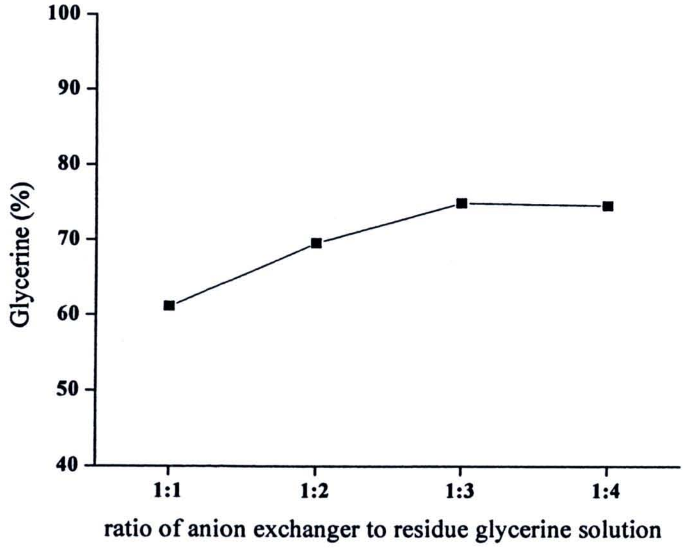

Figure 4.11 Effect of the ratio of anion exchange resin to glycerine on percentage of glycerine content

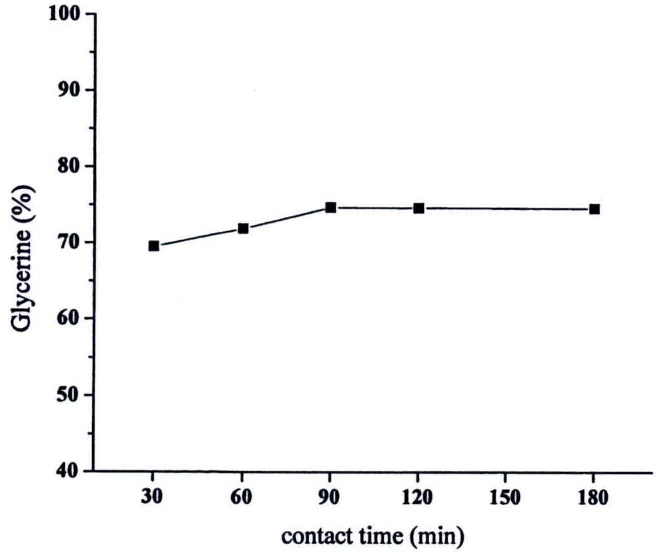

Figure 4.12 Effect of contact time of anion exchange resin to glycerine on percentage of glycerine content

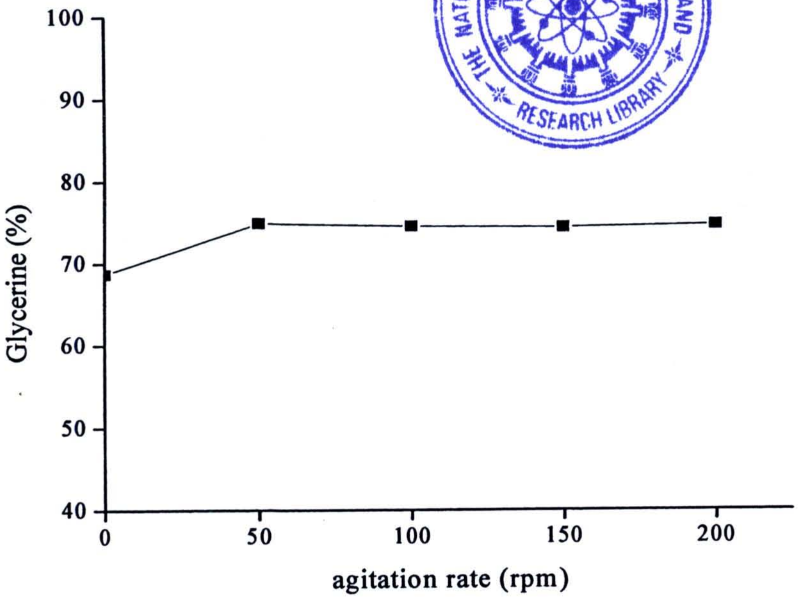

Figure 4.13 Effect of agitation rate of anion exchange resin to glycerine on percentage of glycerine content

Table 4.7 Chemical compositions of purified glycerine obtained from optimized conditions of residue glycerine solution by mixed with anion exchange resin

No. Samples	Glycerine (%)	Ash (%)	Water (%)	MONG (%)	Density (g/cm^3)	pH
1	74.97	10.16	10.01	5.52	1.34	6.79
2	74.53	10.75	9.54	4.79	1.65	6.91
3	74.23	11.13	9.78	5.76	1.32	6.75
Average	74.58	10.68	9.78	5.36	1.44	6.82

FT-IR spectra of standard glycerine and purified glycerine obtained by optimized conditions of residue glycerine solution was mixed with anion exchange resin are expressed as shown in Figure 4.14. The presence of OH group in all samples was evidenced by fundamental mode of O-H stretching at 3387 cm^{-1}. It was found that C-H stretching was at 2890 and 2942 cm^{-1}. The presence of some impurities was present by the absorption peak at 1650 cm^{-1} (C=O group). Furthermore, C-O stretching from 1043 to 1111 cm^{-1} and O-H bending at 924 cm^{-1}

were observed in FT-IR spectra of standard glycerine. FT-IR spectra of purified glycerine obtained from improved method also showed almost similar absorption patterns but represent broader absorption band at 3387 cm^{-1} and 1400-2942 cm^{-1}. This was also probably due to the hydroxyl groups from water and ash content.

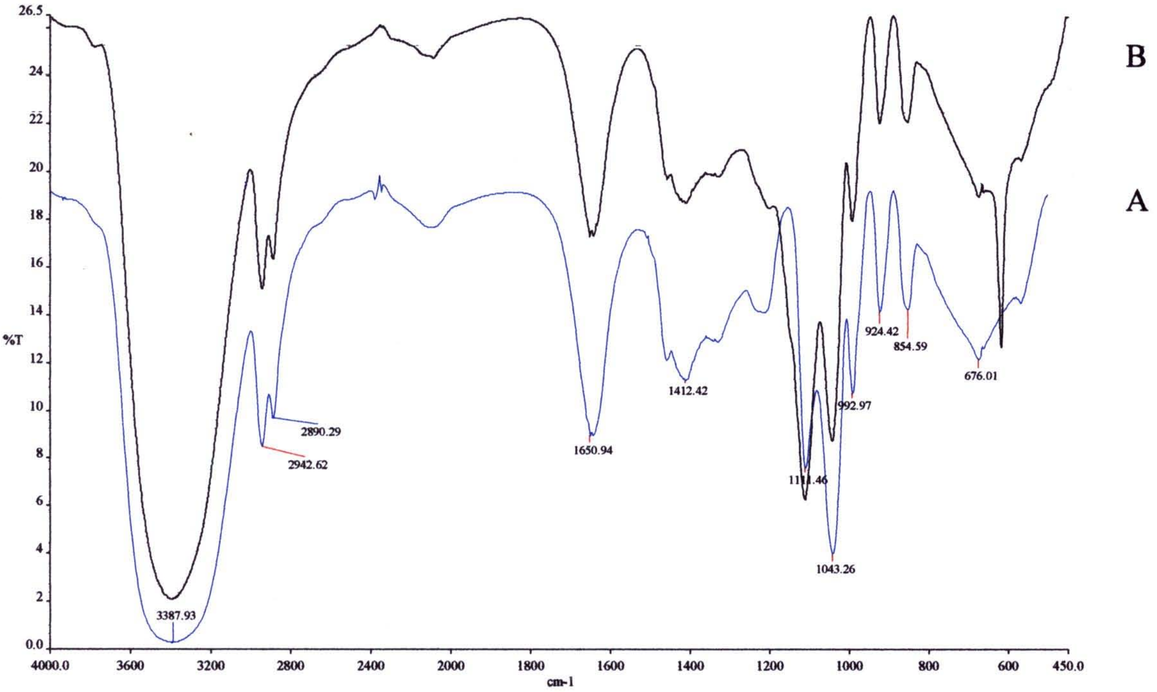

Figure 4.14 FT-IR spectra of standard glycerine (A) and improved method of residue glycerine solution by mixed with anion exchange resin (B)

4.3.2.3 Study of optimization conditions for purification of residue glycerine solution by using mixed cation exchange resin with anion exchange resin

The second parameters were ratio of both cation exchange resin with anion exchanger resin to residue glycerine solution (1:1, 1:2, 1:3 and 1:4 w/w), contact time (30, 60, 90, 120 and 180 min) and agitation rate (0, 50, 100, 150 and 200 rpm). The eluates were then evaporated to remove methanol. The final products were also called purified glycerine. The results of optimization conditions by mixed both cation exchange and anion exchange resin are demonstrated in Figure 4.15 - 4.17. It was indicated that these optimized conditions for batch experiment obtained were 1:3(w/w) of ratio of mixed both cation exchange and anion exchange resin to glycerine, 90 min of contacting time and 50 rpm of agitation rate, respectively. Finally, the purified glycerine in this optimized condition comprised 83.06% glycerine, 6.20% ash, 9.12% water and 1.62% MONG as summarized in Table 4.8.

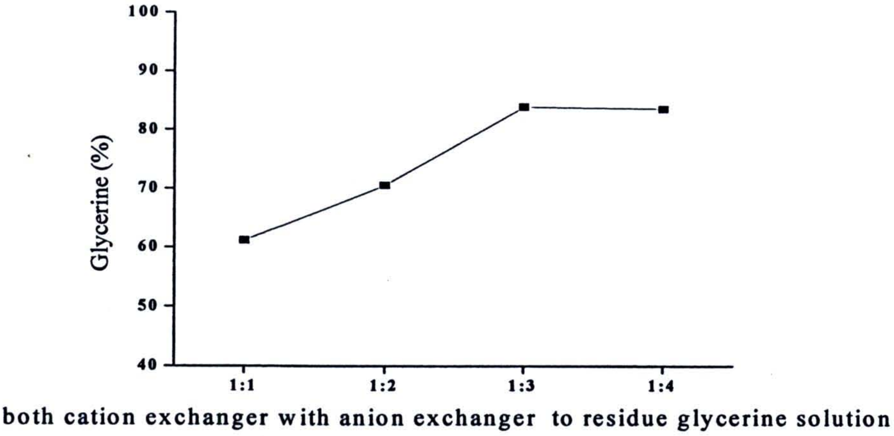

Figure 4.15 Effect of the ratio of mixed both cation exchange resin and anion exchange resin to residue glycerine solution to glycerine on percentage of glycerine content

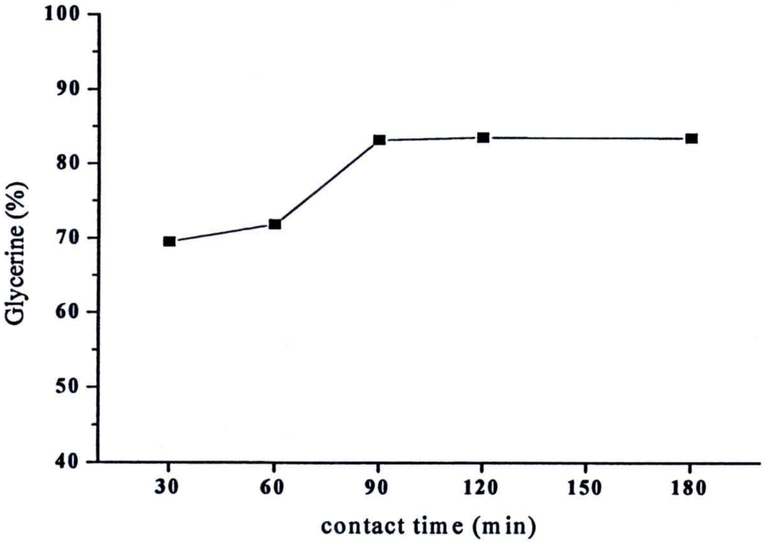

Figure 4.16 Effect of contacting time of both mixed cation exchange and anion exchange resin to residue glycerine solution to glycerine on percentage of glycerine content

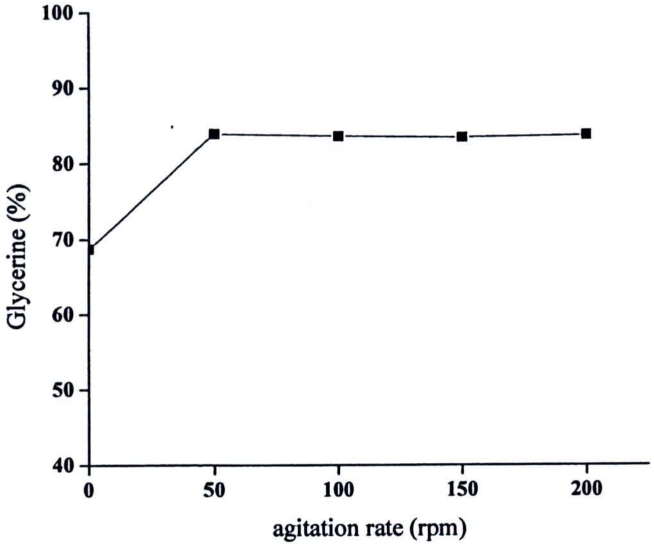

Figure 4.17 Effect of agitation rate of both mixed cation and anion exchange resin to residue glycerine solution to glycerine on percentage of glycerine content

Table 4.8 Chemical compositions of purified glycerine obtained from optimized conditions of residue glycerine solution by mixed with both cation and anion exchange resin

No. Samples	Glycerine (%)	Ash (%)	Water (%)	MONG (%)	Density (g/cm^3)	pH
1	83.12	6.20	9.15	1.65	1.25	6.78
2	82.94	6.22	9.12	1.62	1.26	6.95
3	83.12	6.18	9.10	1.60	1.29	6.59
Average	83.06	6.20	9.12	1.62	1.27	6.77

FT-IR spectra of standard glycerine and purified glycerine obtained from mixed both cation resin and anion exchange resin are expressed as shown in Figure 4.18 The presence of OH group in all samples was evidenced by fundamental mode of O-H stretching at 3399 cm^{-1}. It was found that C-H stretching at 2890 and 2942 cm^{-1}. The presence of some impurities was shown by the absorption peak at 1650 cm^{-1} (C=O group). Furthermore, C-O stretching from 1043 to 1111 cm^{-1}

and O-H bending at 924 cm^{-1} were observed in FT-IR spectra of standard glycerine. FT-IR spectra of standard glycerine and purified glycerine obtained from mixed both cation and anion exchange resin showed almost similar absorption patterns but with a broader absorption band at 1500 to 1200 cm^{-1}, assigned overlapping of C-H in-planes and O-H bending in the glycerine molecule. This was probably due to ash content in purified glycerine (Hazimah et al., 2003).

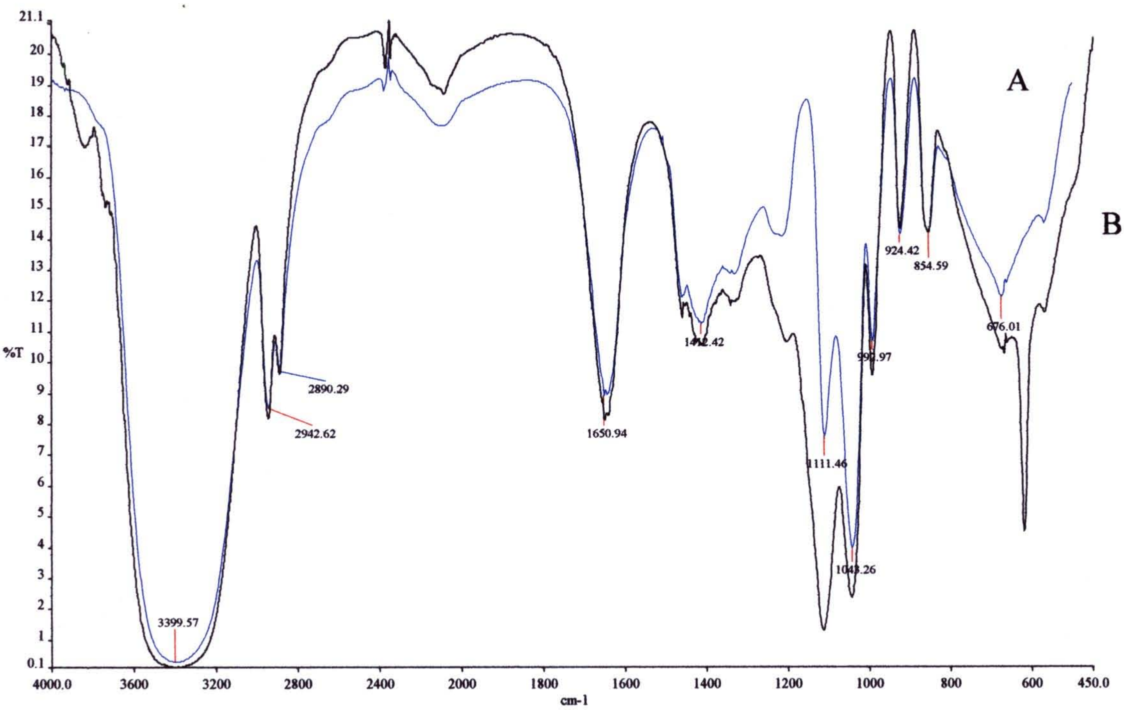

Figure 4.18 FT-IR spectra of standard glycerine (A) and improved method of residue glycerine solution mixed with both cation and anion exchange resin (B)

Table 4.9 Comparison of improved methods by ion exchange chromatography

Methods	Glycerine (%)	Ash (%)	Water (%)	MONG (%)	Density (g/cm^3)	pH
Standard glycerine	99.50	0.01	0.44	0.02	1.25	6.86
Cation exchange resin	74.25	10.95	9.69	5.11	1.23	6.84
Anion exchange resin	74.58	10.68	9.78	5.36	1.44	6.82
Mixed both Cation and Anion exchange resin	83.06	6.20	9.12	1.62	1.27	6.77

The comparison purified of residue glycerine by improved methods was investigated. Several analyses, such as glycerine content, ash content, water content, MONG content, density and pH. The results of comparison are expressed in Table 4.9. The purification by using mixed both cation and anion exchange resin can increase glycerine content. Moreover, ash and MONG content decrease because both cation and anion exchange resin can exchange positive charge ions and negative charge ions from ionization of salts and other impurity, constituted the ash and MONG. Therefore, ash and MONG content was decreased resulting in the higher purity of glycerine was obtained by improved method. Moreover, MONG, which comprised mainly partial glycerides, free fatty acid, oxidation products and the polymerized compounds of glycerine, was reduced.